



Engineering-geological modeling for supporting local seismic response studies: insights from the 3D model of the subsoil of Rieti (Italy)

Antonielli Benedetta^{1,2} · Iannucci Roberto^{1,2,4} · Ciampi Paolo^{1,2} · Martino Salvatore^{1,2} · Marchetti Domenico³ · Giudici Federico¹ · Scarascia Mugnozza Gabriele^{1,2} · Bozzano Francesca^{1,2}

Received: 6 July 2022 / Accepted: 10 May 2023
© The Author(s) 2023

Abstract

A high-resolution 3D engineering-geological model of the subsoil can be derived by integrating stratigraphic and geophysical data in order to represent reliably the geological setting, and therefore support several geological studies such as local seismic response analyses. In this study, we show how an accurate 3D engineering-geological model suggests the proper seismic response modeling approach (1D or 2D) in a peculiar and complex geological context, such as the historical city center of Rieti (Italy), selected as test site, and characterized by important lateral heterogeneities between stiff travertine and alluvial soft deposits. The proposed methodology involves three steps: (i) conceptual geological modelling, obtained from data and maps of literature; (ii) engineering-geological modeling, validated through geophysical data; and (iii) a 3D model restitution achieved by a geodatabase (built basing on the previous steps), that collects, stores, reliably represents, and integrates properly the geospatial data. The analysis of seismic ambient noise measurements specifically available for the study area allowed to infer the shear wave velocity value for each lithotechnical unit and to retrieve some additional stratigraphies. These synthetic log stratigraphies allowed to improve the detail of the geodatabase and therefore a more accurate 3D geological model. Such a reliable engineering-geological model of the subsoil is required to perform a site-specific seismic response characterization which is a fundamental tool in the framework of seismic risk management.

Keywords Engineering-geological model · Site effects · 1D and 2D seismic response · 3D solid model · Travertine

Introduction

In recent decades, integrated approaches based on engineering-geological modeling, geophysical investigations, and numerical modeling were developed for the evaluation of the seismic shaking expected in a given site in the framework of local seismic response and seismic microzonation studies. The resolution of local seismic

response studies is directly related to the accuracy of the engineering-geological model, as it allows to evaluate the expected seismic site effects and consequently leads to the choice of the proper approach (e.g., 1D or 2D) of the seismic wave propagation modeling to be used. These numerical approaches simulate the propagation of seismic waves from the seismic bedrock to the surface and are strictly related to the physical and mechanical properties of soils as well as to the geometrical features of topography and buried geological bodies. In this regards, previous studies evidenced as a 2D modeling approach could reliably simulate the seismic wave propagation and assess the seismic motion amplification in the case of strongly heterogeneous alluvial valleys (Gaudiosi et al. 2014; Martino et al. 2015; Macerola et al. 2019; Pergalani et al. 2020; Varone et al. 2021) or volcanic filling deposits (Moscatelli et al. 2021) as well as topographic reliefs (Antonielli et al. 2021). On the other hand, a 1D modeling approach resulted able to simulate the seismic motion amplification in sites characterized by a subsoil that can be assumed as mainly composed of planar,

✉ Antonielli Benedetta
benedetta.antonielli@uniroma1.it

¹ Department of Earth Sciences, Sapienza University of Rome, P.Le Aldo Moro 5, 00185 Rome, Italy

² CERI—Research Centre for Geological Risks, Sapienza University of Rome, P.Le Aldo Moro 5, 00185 Rome, Italy

³ Studio Geologico Marchetti, Via Della Chimica Snc, 02100 Rieti, Italy

⁴ ANSFISA National Agency for the Safety of Railways and Road and Motorway Infrastructures, P.le dell'Industria 20, 00144 Rome, Italy

homogeneous, and subhorizontal strata (e.g., Sonmezer et al. 2019; Tunar Özcan et al. 2019; Iannucci et al. 2022), where the bidimensional seismic effects related to lateral variations are negligible.

The 3D engineering-geological modeling depicts the geological structure in detail and the spatial distribution of available parameters, representing an effective tool for visualization, analysis, and integration of information (Baojun et al. 2009; Liu et al. 2020). Several applications of the model are possible at different scales and include hazard zoning, land use planning, and management activities or the structural maintenance of buildings (Guo et al. 2021). The 3D engineering-geological modeling includes the interpolation of geological and geotechnical data and is based on a conceptual geological model, generally consisting of a series of geological cross sections, elaborated starting from the maps and data available in the literature, from borehole data and geophysical measurements, and that is above all from punctual information (Aghamolaie et al. 2019).

The 3D modeling provides several advantages in understanding the geological and structural setting of the subsoil; in fact, all the geological data are integrated thus obtaining an overview that helps to visualize the relationships between the lithologies (He et al. 2020). The solid models also make it possible to provide a representation of geological setting both on the surface and in-depth, which would not be interpreted through more traditional approaches, generally due to lack of extensive and pervasive information (Royse et al. 2009). General shortcomings of 3D engineering-geological models lie in the limitations of modeling procedures and software, and that is the modeling results may not reflect the intrinsic property, heterogeneity, and anisotropy of subsurface parameters. In particular, modeling softwares are not well suited for small- to medium-sized sites, while they are more effective for investigating large study areas and demonstrating relationships between geological strata and properties on a macroscopic scale. These sites require more specific research to fully comprehend the inherent variability of complex geobodies (Zhu et al. 2013). The level of geological detail in the model is directly linked to the quantity and quality of digital data, such as accurately logged boreholes and downhole geophysics data. Classical modeling techniques may also struggle with stratal pinch-out phenomena (Royse et al. 2009). To address these limitations, a sequential, multisource modeling approach can reconcile geological and geophysical data, capture high-resolution characterization of subsurface hydrogeophysical properties, and establish coupling relationships between geological structures and property parameters (Ciampi et al. 2022; Zhang and Zhu 2018).

This study aims at restituting a 3D geological model of the subsoil of Rieti to describe accurately where local amplification effects may occur in the case of seismic shaking and to suggest zones where a 2D seismic response

modeling approach should be preferred with respect to the 1D one. The Rieti area is indeed considered to be of medium–high seismicity, and it was affected by destructive seismic events such as the 1898 earthquakes (Comerci et al. 2003; Colombi et al. 2011).

The ancient Roman city of Rieti (formerly known as *Reate*) was developed on the southeastern edge of the intermontane basin of the Central Apennines (Central Italy), at the confluence of two rivers, Turano and Velino. It was built on a small cliff of continental carbonate deposits produced by cold mineralized waters (calcareous tufa), commonly called “travertines” which were then deeply engraved by the hydrographic network and karstified. Over the centuries, the growth of the city led to the stratification of the Roman, then medieval and subsequent eras ruins, up to the present day, covering and hiding the slopes of the travertine cliff. Therefore, under the current city, there is now a layer of variable thickness (with a maximum of 15 m) of backfill deposits due to the long and intense urbanization of this area.

The lithoid travertine platform is a highly competent rigid lithological body, with an elongated shape in the EW direction (which extends about 1.2 km in the EW direction and 240 m in the NS direction), surrounded by the soft alluvial sediments of the Velino valley (Guerrieri et al. 2006; Archer et al. 2019). This peculiar geological setting can have implications regarding the seismic risk of the Rieti city due to possible local seismic motion amplification effects and earthquake-induced deformation phenomena.

This study has been developed in the framework of the H2020-RISE “STABLE” (Structural stABLity risk assEsment) project (www.stable-project.eu; Serpetti et al. 2020), which concerns the cultural heritage protection in the peri-Mediterranean area and in particular the evaluation of the action seismic on some buildings of historical and cultural interest in the Mediterranean basin, through the construction of geological models of the subsoil, evaluation of expected seismic shaking, and vulnerability analysis of the historic buildings.

An estimation of the expected ground motion based on site-specific local seismic response studies is crucial to mitigate the seismic risk. In this regard, following the 2016–2017 seismic sequence and the subsequent Italian National Government Decree OPCM 24/2017, seismic microzonation (SM) studies were carried out in 138 municipalities of Central Italy (Moscatelli et al. 2020) according to the Italian National Guidelines (ICMS Working Group 2008). The level 3 seismic microzonation (SM) study produced for the municipality of Rieti (<https://sisma2016data.it/microzonazione/>) identified several zones with expected homogeneous effects in the case of earthquakes and fixed a base seismic hazard with a probability of exceedance of 10% in 50 years (i.e., a return period of 475 years), provided acceleration time histories and elastic response spectra

representative of the expected ground motion at the surface for each zone based on 1D simulations.

Historical background of the Rieti city

The foundation of the city of Rieti, the ancient Reate, the capital of Sabina, can be placed at the beginning of the Iron Age, and antiquarian historiography recognized the eponymous divinity Rhea as its founder. In 290 BC, the city was definitively assimilated into the Roman Empire thanks to the conquest of the consul Manio Curio Dentato, who promoted the drainage of the Rieti plain, until then occupied by the waters of Lake Velinus (Alvino and Lezzi 2013; 2016). This important hydraulic engineering work was carried out through channeling and cutting of the barrier (as natural dam of travertine incrustations) which caused the formation of the lake itself and gave rise to the cascade now known as the Falls of Marmore (Madonna et al. 2020). This work was appreciated for its landscape effects, and it increased the agricultural production in the Rieti valley, but it caused also conflicts between Reate and Interamna, the current Terni city, due to the consequences of water regulation of the Velino river.

The primitive nucleus of the city stood on the travertine hill to the right of the Velino river, and was located in a sparsely populated but rather rich region, and the city maintained the rank of prefecture until the Augustan age, when it became a municipium. Under the Flavian dynasty, that was originally from Sabina, Rieti went through a period of prosperity, which lasted until the late imperial age (Alvino and Lezzi 2013; 2016). The Roman city, whose plan and perimeter are nowadays still easily recognizable, was organized according to typical Roman urbanistic standards, in square allotments and two main orthogonal roads, the decumanus, which represented the ancient main road in east–west direction (today Via Cintia–Via Garibaldi), and the cardo (today Via Roma), that make up the settlement’s backbone and was fortified with strong walls (Alvino and Lezzi 2013; 2016).

A stone bridge was laid across the Velino river, and a large viaduct was built to bring goods from the via Salaria—the ancient road, first used by the Sabines to transport salt from the salt marshes at the mouth of the Tiber directly to Rieti’s southern door (Madonna et al. 2020). During the early Middle Ages and Middle Ages, the bridge, the walls with its towers, and the road network of the ancient city were preserved (Alvino and Lezzi 2013; 2016).

In the early Middle Ages, Rieti, that was legally established as a Diocese in the fifth century, was annexed to the Duchy of Spoleto City. Due to its strategic position on the border with the Kingdom of Naples, Rieti became one of the seats of the papal curia, hosting some popes for long periods. The presence of the papal court led to a significant

increase in population during the thirteenth century, leading the municipality to decree in 1252 the expansion of the walls and the urbanization of the plain surrounding the travertine hill. Valuable noble palaces and churches were built in this period, such as the Romanesque cathedral of Santa Maria Madre di Dio, rebuilt between 1109 and 1225 on the remains of the primitive early Christian Basilica, and the monumental papal palace built between 1283 and 1288. Rieti remained faithful to the papal state until the beginning of the Risorgimento period.

Geological setting

The city of Rieti is located in the southern part of the homonymous intermountain basin of the Central Apennines, which is a Plio-Pleistocene extensional depression with a subrectangular geometry due to the action of NS and EW normal faults (Patacca et al. 1992; Cosentino and Parotto 1992; Doglioni 1993; D’agostino et al. 2002). The Rieti basin is surrounded by outcropping pelagic units and carbonates of the Meso-Cenozoic platform, and flysch sediments of the Miocene Apennine foredeep (Guerrieri et al. 2006; Archer et al. 2019).

Since the Upper Pliocene up to the Lower Pleistocene, the basin was filled with a fluvio-lacustrine sequence 0.5–2 km thick (Cavinato and De Celles 1999), represented by fluvial deposits, alluvial fans, and lacustrine sediments attributed by Guerrieri et al. (2004) to two main depositional units (UPL and LPL), separated by an erosive surface. At the end of the lower Pleistocene, a regional tectonic uplift affected a major part of the Central Apennines (Blumetti et al. 1993) and new direct faults, striking NS and EW, were activated in the Rieti basin, which it assumed its present form in the Middle Pleistocene. The ultra-basic volcanism of the small town of Cupaello and Polino along the eastern edge of the basin is also connected to this extensional phase (Stoppa and Villa 1991; Carminati et al. 2012; Lustrino et al. 2022).

The “Rieti fault” trending NW–SE and dipping SW, which represents the eastern boundary of the basin, was active until the Holocene: paleoseismic analyses (Michetti et al. 1995) showed that between 5000 and 6400 BP, the fault is capable to produce M 6.5 earthquakes and surface faulting (Madonna et al. 2020).

Moreover, the depocenter of the sedimentary basin moved to the NW, and this led to the recall and capture of numerous river axes that affect their own deposits. Consequently, the Villafranchian River network of the Rieti and Terni basins was rejuvenated and the Velino River deviated towards NNW (Michetti et al. 1995; Madonna et al. 2020).

The climatic variations that occurred from the Pliocene up to the entire Quaternary, and in particular the alternating glacial and interglacial phases and fluctuations in the level

of the base aquifer, caused karst phenomena that affected the Meso-Cenozoic carbonates outcropping at the basin footwalls (Calderoni et al. 1994). In addition to the prevailing action of climate, tectonics and the ascent of deep fluids also had significant effects on the chemistry of the waters. The latter then alternated phases in which they were strongly encrusting, leading the formation of continental carbonate deposits, and phases in which they were highly erosive, during which karst processes were favored.

The Rieti basin hosted a lake with variable extent that resulted in high stands and triggered the growth of travertine platforms during the Holocene “warm” fluctuations. In these interglacial phases, the four lakes occupying the drainage basin (called Lungo, Ripasottile, Ventina, and Piediluco) were joined to form a large water basin, the so-called “Lacus Velinus,” that extended throughout the Rieti basin up to the Le Marmore threshold located at the northwestern edge of the basin (Ferrelì et al. 1992; Carrara et al. 1995; Calderini et al. 1998). Le Marmore Falls are a large waterfall whose top surface is 375 m a.s.l., formed by an active travertine platform. Such continental carbonates, generically defined as travertines, were deposited along the Velino valley and throughout the Rieti basin in fluvial-lacustrine systems (Brunamonte et al. 1993; Carrara et al. 1992, 1995; Lorenzoni et al. 1993; Michetti et al. 1995; Soligo et al. 2002; Madonna et al. 2020), and consist of porous, bio-induced, and bio-sustained microcrystalline deposits, precipitated as encrustations on the aquatic vegetation starting from karst mineralized waters and can be classified as calcareous tufa (Pedley et al. 2003; Gandin and Capezzuoli 2008; Capezzuoli et al. 2008; Arenas-Abad et al. 2010; Madonna et al. 2020) (Fig. 1).

In the Rieti city area, a Middle Pleistocene travertine plate was formed, surrounded, in the southernmost zone of the basin, by a fluvial-lacustrine succession, and is currently attributable to depositional processes of the Velino River. At the Rieti city center, the outcropping travertines are represented by lenticular subhorizontal banks of limestone characterized by an irregular alternation of bio-induced high porosity facies, and by more homogeneous, fine, and compact facies (Fig. 2). There are also sands and reddish residual carbonate silts (“red soils”). The organic content in the more porous facies is represented by accumulations of plant remains and limestone muds with encrusted remains of both aquatic and terrestrial invertebrates. These facies and their associations are characterized by stepped sections, between tanks delimited by phytohermal dams (fluvial barrages) filled with calcareous mud and silts deposited in small lakes and ponds. North of the city center, a further travertine complex with different lithological characteristics crops out widely. This formation is characterized by more

levels with loose silty sands and clayey, and it has been defined in the literature as “detrital travertine” (Scarascia Mugnozza et al. 2013).

Gravimetric investigations (Scarascia Mugnozza et al. 2013; Skrame et al. 2018) allowed to estimate the thickness of the travertine platform of the Rieti. Through the study of the gravimetric anomalies, and the trend of the thicknesses of the lithologies by calculating the density, a thickness of about 40 m has been evaluated for the travertine plate of the Rieti city center.

Similarly to other Apennine intermontane basins, the one of Rieti is typically characterized by a thick succession of continental clastic sediments, with an overall thickness of 400–500 m (Guerrieri et al. 2004; Carrara et al. 2004; Camerieri 2009; Camerieri and Mattioli 2014). The deposits are essentially made up of fluvial lacustrine sediments, but at depth, the succession becomes more complex and reflects different phases in which a marked erosion occurred alternating with depositional phases during the Quaternary.

Calderini et al. (1998) proposed a reconstruction of the different phases of climatic fluctuation that affected the westernmost part of the Rieti basin, following the last glacial phase, in a time window that goes from the Middle Pleistocene, when the plain underwent a tectonic subsidence, up to the Upper Quaternary:

- From the late Pliocene, Early Pleistocene, there is an alternation of laminated limestone with alluvial fan conglomerates, gravels, and gravelly sands, with well-rounded clasts. Above, there are gravel levels, silty arenaceous levels, sands with organic matter, and sometimes peaty vegetables deriving from the depositional phases in a braided fluvial plain
- In Middle Pleistocene, sandy and sandy-clayey volcanoclastic layer rich in biotite, muscovite, and pyroxene, due to the volcanic activity of Cupaello, occurred during the tectonic collapse of the Rieti basin; deposition of the travertine platform in the Rieti area
- From the Late Pleistocene to the Lower Holocene, clays with calcareous fragments with aquatic mollusks and ostracods that testify to the presence of freshwater from shallow basins, with a progradation of alluvial fan from nearby escarpments
- From about 6000 to 2700 years ago, clays with peat deposited in shallow lake waters or ponds rich in vegetation following the decrease in the base water level during a global cooling event
- Fine-grained sediments rich in mollusks and ostracods during the subsequent new water level rise
- Clays with hydrophilic organisms (land mollusks) deposited during the last progressive drying up of the Rieti

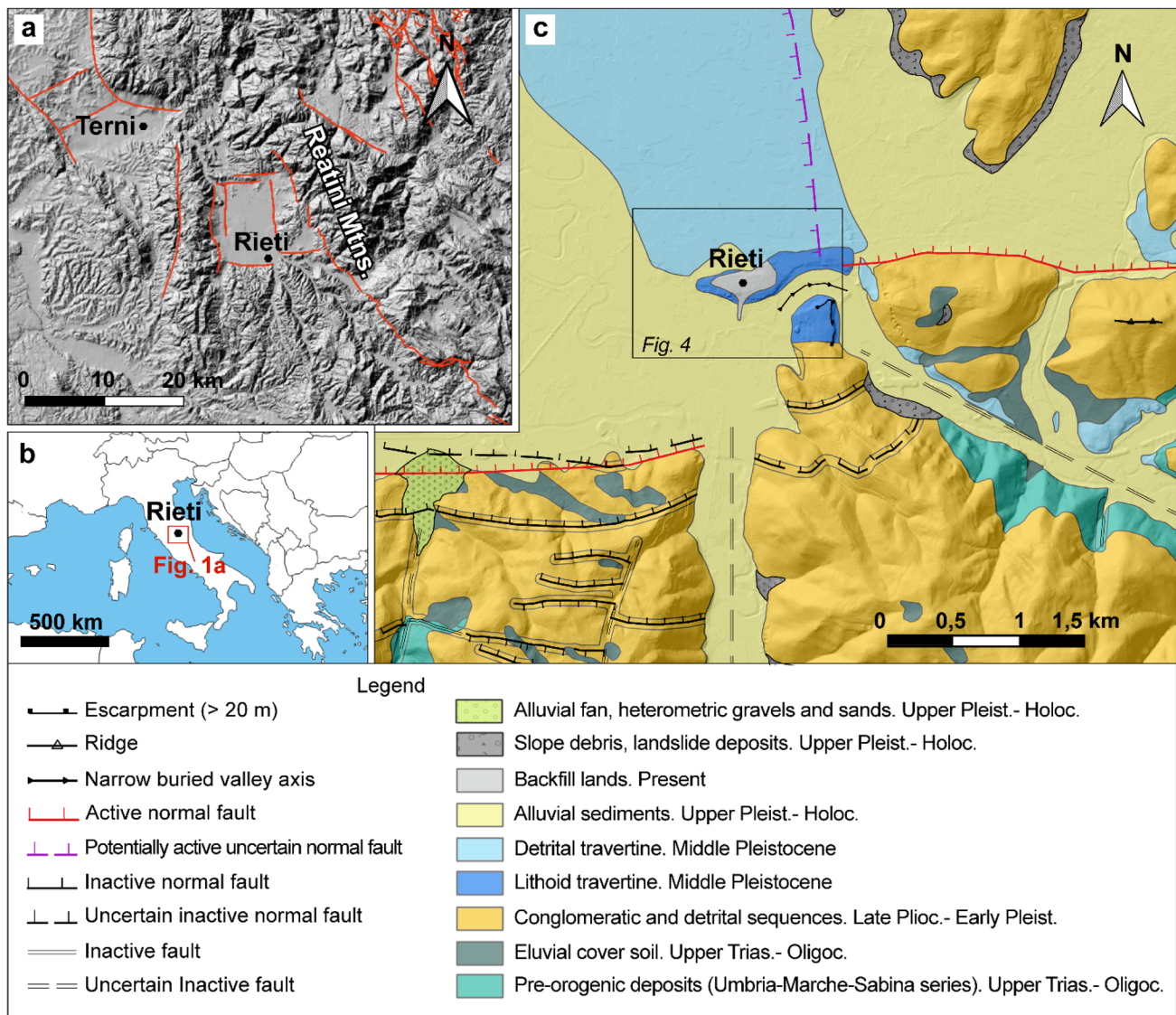


Fig. 1 Geological setting of the study area: **a** Rieti basin and active faults from ITHACA (ITaly HAZards from CApable faults) catalog (ITHACA Working Group 2019), **b** location of the study area: red

box corresponds to the map area shown in a; and **c** lithotechnical units from level 1 MS study

plain, up to the current alluvial sediments of the Velino and Turano Rivers.

The depositional sequence of the Velino River is characterized by an alternation of silty sands, mixtures of sand and silt, and layers and lenses of gravel, peat, and inorganic silts, of an intermontane basin environment; in these sections, however, the geological bedrock was not reached (Scarascia Mugnozza et al. 2013).

Earthquakes which occur in this sector of the Central Apennines are frequent and generally occur as multiple-shock sequences with relatively shallow hypocenters

(< 12 km below the land surface; Rovida et al. 2022). The mainshocks of the seismic sequence of the Central Apennines of 2016–2017 that activated fault segments (Laga Fault, Vettore and Monte Bove Fault; Chiaraluce et al. 2017; Galli et al. 2017) caused a maximum intensity of V MCS (Mercalli-Cancani-Sieberg scale) at Rieti (Galli et al. 2017).

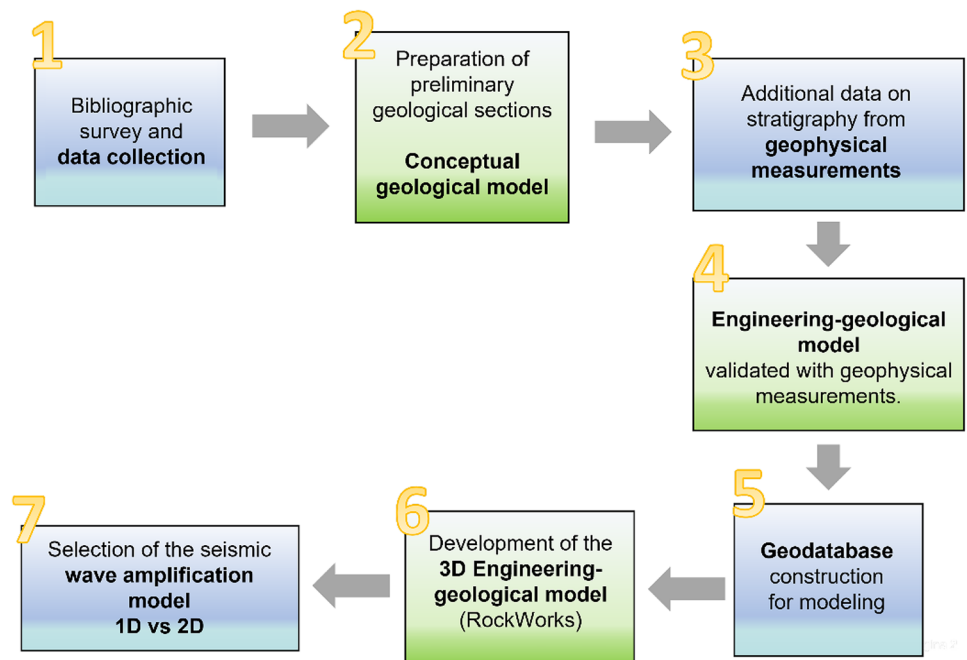
The Rieti area is included in a medium-to-high seismicity zone, with a seismic history characterized by at least 22 earthquakes that occurred in historical times (from the year 1000 to present day) which affected the city with a macroseismic intensity > V MCS, and 4 of these latter with intensity VIII (Locati et al. 2022). The Mw 5.3 earthquake



Fig. 2 Lithoid travertine (calcareous tufa, sensu Madonna et al., 2021) outcropping in Rieti: **a, b** travertine platform outcropping in the historic center; **c, d** piece of a core drilled in the center of Rieti, near the town hall; and **e** travertine outcrop at the base of an ancient building, in the historic city center

of June 27, 1898, with the epicenter near the city, was the most destructive of the historical times, together with the earthquake of 1298, and caused the damage to most of the

Fig. 3 Flow chart of the work addressed in this study



buildings in the historic center and the collapse of some (Comerci et al. 2003; Colombi et al. 2011; 2013; 2015).

Methods

In this study, 31 borehole logs, 3 downhole surveys, 3 MASW tests, and 5 high-quality HVSr curves according to SESAME (2004), as well as the geotechnical map belonging to the level 3 SM study conducted for the Rieti Municipality in 2017, have been used.

The main steps of this work are represented in the flow chart in Fig. 3. The stratigraphy of the available surveys was analyzed (step 1) to produce detailed geological cross sections of the historic center of Rieti. These cross sections represented the preliminary geological model of the study area (step 2).

In order to increase the information needed to reconstruct a detailed stratigraphy, geophysical investigations (i.e., downhole, MASW, and HVSr survey results) were also used to obtain additional stratigraphic columns using an inversion procedure with an iterative approach (step 3); these extrapolated stratigraphic columns have been merged into the geodatabase to obtain the subsequent 3D model.

The geophysical measurements also made it possible to validate the previously elaborated geological cross sections, allowing the definition of an engineering-geological reference model (step 4), needed for the construction of the geodatabase. Geological data stored in the geodatabase have been interpolated (step 5) using RockWorks software, in order to visualize the engineering-geological model in three dimensions (step 6). Such visualization makes clear

the identification of the zones where there is an impedance contrast between the substrate or stiff rocks and cover soft sediments (step 7), where seismic waves amplification phenomena can occur.

The preliminary geological model has been elaborated through 5 geological cross sections that resulted from the analysis and interpolation of the borehole logs, and of the geophysical data (location in Fig. 4), as well literature survey and in particular on (i) the study by Calderini et al. (1998) about the sediments of the Rieti plain and (ii) the gravimetric study by Scarascia Mugnozza et al. (2013) and Skrame et al. (2018), which determined the thickness of the travertine plate and the thickness of the deposits in the Rieti area. Some assumptions were necessary for areas not well covered by the boreholes and at depths greater than 15 m, due to the shallow depths reached by most of the stratigraphic logs (13 shallow logs). Only 9 boreholes got to 30 m depth, and only 1 borehole, located in the easternmost part of the study area, reached 40 m of depth.

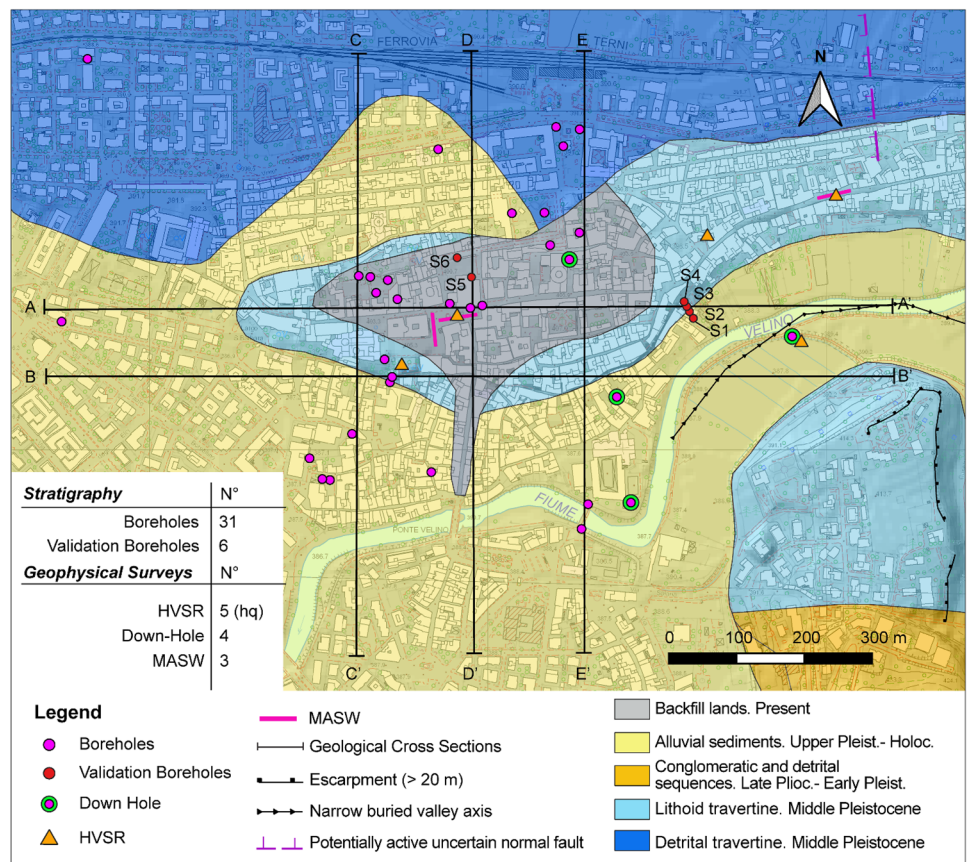
Following a preliminary reconstruction of the geological model, an inversion procedure with an iterative approach was performed using the 5 high-quality HVSR curves to validate the preliminary cross sections and calibrate its parameters as follows: (i) the range of values of the main physical and mechanical parameters were defined for each

Table 1 Litotechnical units identified for the Rieti historical center area and relative Vs values calibrated by the HVSR inversion

Litotechnical unit	Vs (m/s)
Backfill deposits	140
Backfill deposits with travertine clasts	350
Clayey silts	175
Silty sands with calcareous clasts	160
Gravels	220
Silty sands with peat	210
Sandy silts and clays	280–300
Sands with organic matrix	400
Gravelly sands in silty matrix	730
Gravels and gravelly sands	820
Reddish and brownish clays	150–310
Sandy and silty clays	250–280
Sandy travertine	400–570
Travertine	700–830

lithological unit identified in the preliminary model using the reports of field surveys and laboratory tests, with a particular focus on shear-wave velocity (Vs) values contained in downhole and MASW reports; (ii) considering the preliminary model, the 5 sites of seismic ambient noise

Fig. 4 Location of boreholes and geophysical surveys used in this study; the location (traces) of geological cross section is also reported



measurements (location on Fig. 4) outputted high-quality HVSR curves were projected on the cross sections and a stratigraphic log was extracted for each site; (iii) the empirical relationship of the site resonance frequency was used to validate the stratigraphic log obtained for each site and the V_s values of the composing layers.

The horizontal-to-vertical spectral ratio (HVSR) method by Nakamura (1989) consists in estimating the ratio between the horizontal (H) and vertical (V) Fourier amplitude spectra components computed for a set of natural frequency values on recordings of single-station seismic ambient noise. This method allows the evaluation of the site resonance frequency (f_0) identified by a clear peak in the HVSR function, especially where a soft soil topmost-layer generates a marked shear-wave velocity contrast with the underlying seismic bedrock (Bour et al. 1998; Haghshenas et al. 2008), with a resonance frequency value strictly related to the thickness and the shear-wave value of the soft soil layers (Tallini et al. 2020). Considering the capability of seismic measurements in studying the subsoil indirectly, the inversion of their results allows assessing the main parameters needed for seismic applications (Kanli et al. 2006, 2008; Kanlı 2010).

According to experimental data (Oubaiche et al. 2012), the f_0 value can be obtained roughly by the empirical relationship

$$f_0 = \frac{V_s}{4H}$$

where V_s is the mean shear-wave velocity value of the resonant layer and H its total thickness.

Considering a resonant multilayering deposit composed of different layers of soft soils characterized by different shear-wave velocity values, the V_s value can be computed as equivalent velocity obtained using a thickness-averaged relationship (Madera 1970):

$$V_s = \frac{\sum V_{s_i} \times h_i}{\sum h_i}$$

where V_{s_i} is the shear-wave velocity value of the single i th layer and h_i its thickness.

As $\sum h_i$ is equal to H , the f_0 value in the case of resonant multilayering deposit can be assessed roughly as

$$f_0 = \frac{\sum V_{s_i} \times h_i}{4H^2}$$

In the light of this, the iterative approach was performed by varying the V_{s_i} value (according to the ranges defined by the collected material) and, if necessary, the thickness (fixed based on the stratigraphic logs extracted from the preliminary geological model) for each i th layer, until obtaining a correspondence between the theoretically computed f_0 value and the f_0 value obtained on-site by the HVSR analysis.

This procedure allowed to validate the thickness of all the litotechnical units composing the preliminary model, even modifying thickness values of single strata if necessary, obtaining a validated geological model. In addition, a V_s value was calibrated and assigned to each litotechnical unit composing the model (Table 1).

These extrapolated stratigraphic columns were then merged into the geodatabase to obtain the 3D geological model by the procedure explained in the following part.

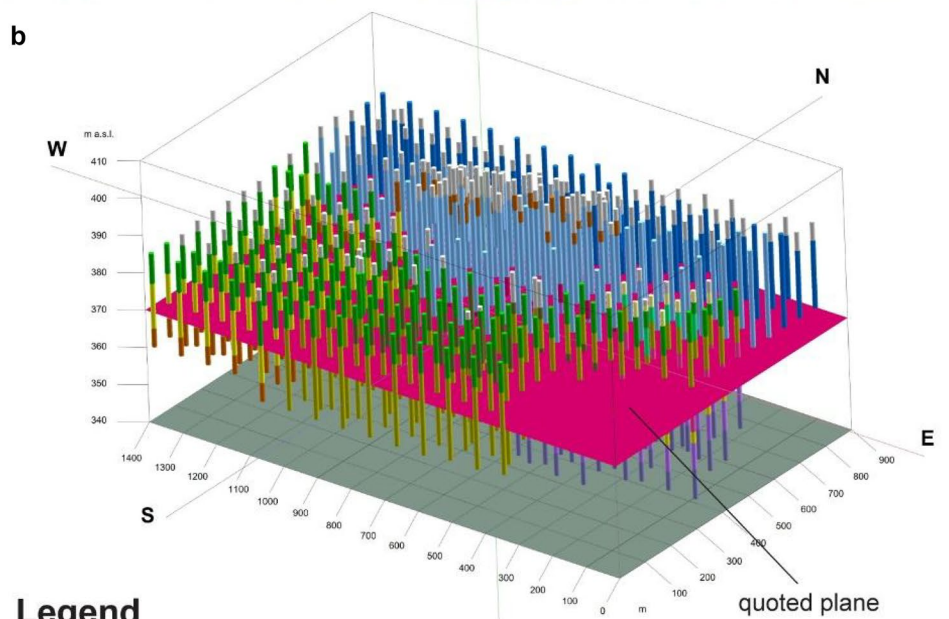
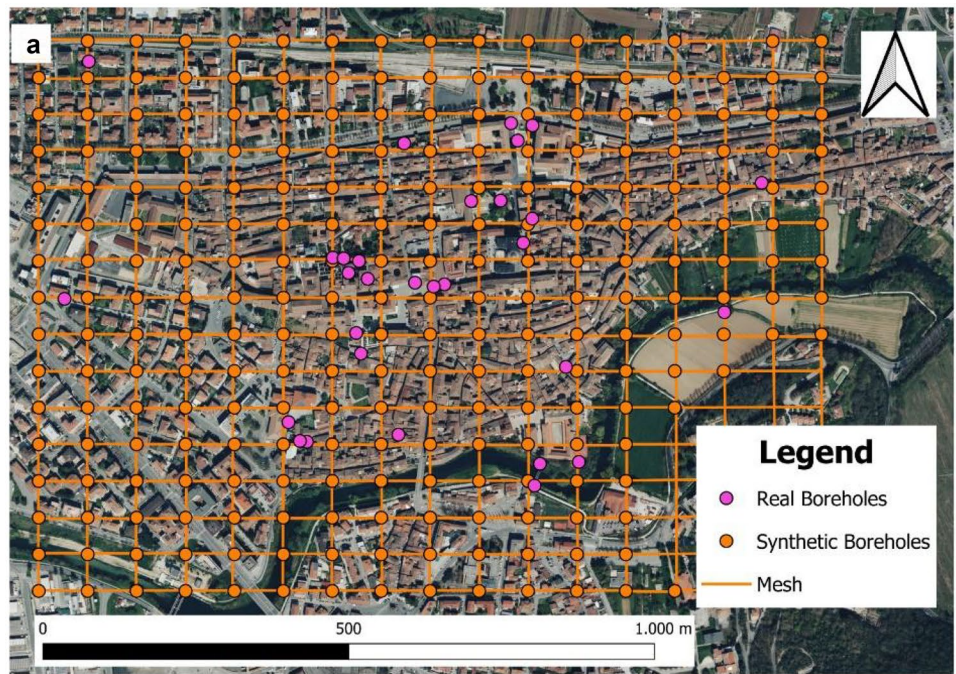
Several “synthetic boreholes” were extrapolated from the geological model that was validated through geophysical investigations. Interpretation of these synthetic boreholes was based on cross sections, geological maps, and information from the literature. This interpretative process was constructed starting from a regular cell grid with dimensions of 80 m × 60 m that covers the study area. Each node of the grid is associated with a specific lithology, according to the geological model, i.e., considering the closest geological cross section. This operation is repeated every 5 m of depth, building several overlapping horizontal grids (quoted plans). As a result, each node of the grid can be considered a discretized synthetic borehole with a vertical sampling step of 5 m.

Discretization into rectangular meshes resulted in the generation of 248 artificial boreholes (synthetic stratigraphies) that were added to the 31 real boreholes, 4 down-hole stratigraphies, 3 MASW test logs, and 5 stratigraphies by HVSR inversion performed in the study domain, covering an area of 116 ha (Fig. 5a). Information associated with these stratigraphies was stored within a multiple Excel spreadsheet.

The latter constitutes a relational geodatabase of geo-referenced data that was employed for processing and editing operations via RockWorks 17 software (Fig. 5b; Ciampi et al. 2021).

Interpolation of the geologic parameters associated with the synthetic boreholes allowed the reconstruction of the surfaces of the stratigraphic contacts. The inverse distance weighting (IDW) method was employed as the interpolation algorithm, using 4 neighboring points and a weighting exponent equal to 2 (Liu et al. 2020). Also, a high-fidelity filter to honor the measured value at the control points and smoothing on the surfaces were used. Stratigraphic contacts isolated the different geologic bodies in the domain of a block model, leading to the generation of a three-dimensional solid model for reconstructing the stratigraphic setting of the subsoil. The use of a three-dimensional mesh consisting of voxels allowed the representation of complex geological structures (Baojun et al. 2009; Ciampi et al. 2021). The domain extends from 407 to 437 m above sea level, and the voxel resolution corresponds to 10 m in the x and y directions, and 0.5 m in the z direction. The 3D solid model results in 130 × 91 × 145 voxels in the x , y , and z dimensions, respectively. The model was used as an interface to extract the stored information at the portions of interest in the spatial domain, and it has

Fig. 5 **a** Synthetic and real boreholes location in the Rieti city and grid mesh architecture. **b** 3D representation of the synthetic and real boreholes with overlapping of a quoted plane (purple) with an elevation of 370 m above sea level for sampling and extraction of the geological data



Legend

Stratigraphy

Backfill deposits	Clays and sands	Clayey silts
Clays and silts	Silty clays	Sands with organic matrix
Clayey silts	Silty sandy clays	Gravelly sands in silty matrix
Silty sands	Silty and clayey sands	Gravels and gravelly sands
Gravels	Lithoid travertine	
Silty sands with peat	Detrital travertine	

the goal to provide a qualitative comparison in reconstructing the geological model using a traditional and a modeling approach.

Results

A validated geological model, composed of 3 geological cross sections with NS orientation and 860 m length, and 2 cross sections with EW orientation and 1200-m length (Fig. 6), was elaborated using the information from literature, 31 borehole logs, and 5 HVSR-inverted stratigraphies used as synthetic boreholes.

The stratigraphic units of the study area were reconstructed by merging the lithologies crossed by the boreholes, under an expert judgment approach and following the information from the literature. The WE cross-section A-A' (Fig. 6) can be taken as a reference for the description of stratigraphic units: at the base, there are gravels and gravelly sands, in a silty matrix, respectively, of the Upper Pliocene and Lower Pleistocene ages, which can be considered as seismic bedrock

as they present V_s values of 730–820 m/s according to the geophysical data collected and confirmed by the model calibration and validation operations. Above these gravels (and below the travertine platform), a level of clays and sands with V_s values of 250–280 m/s was hypothesized (dashed limits in the cross-section A-A' of Fig. 6) since the presence of a clear resonance peak in the HVSR functions obtained by the seismic ambient noise measurements performed on the top of the travertine platform. According to this interpretation, the lithoid travertine platform of the Middle Pleistocene, which presents V_s values from 400 to 830 m/s based on the prevalence of sandy travertine layers, would lie above this soft soil level, and is bordered by alluvial sediments.

In the easternmost sector of the A-A' cross section, the travertine platform was completely eroded by the Velino River. This erosive gap was filled by post-Middle Pliocene sediments starting from sands with organic matter, alternations of clayey silts, silty sands with peaty vegetables, lenses of gravels or gravelly sands referred to river bars, and lastly silty sands and clayey silts, from the Upper Pleistocene to the Holocene.

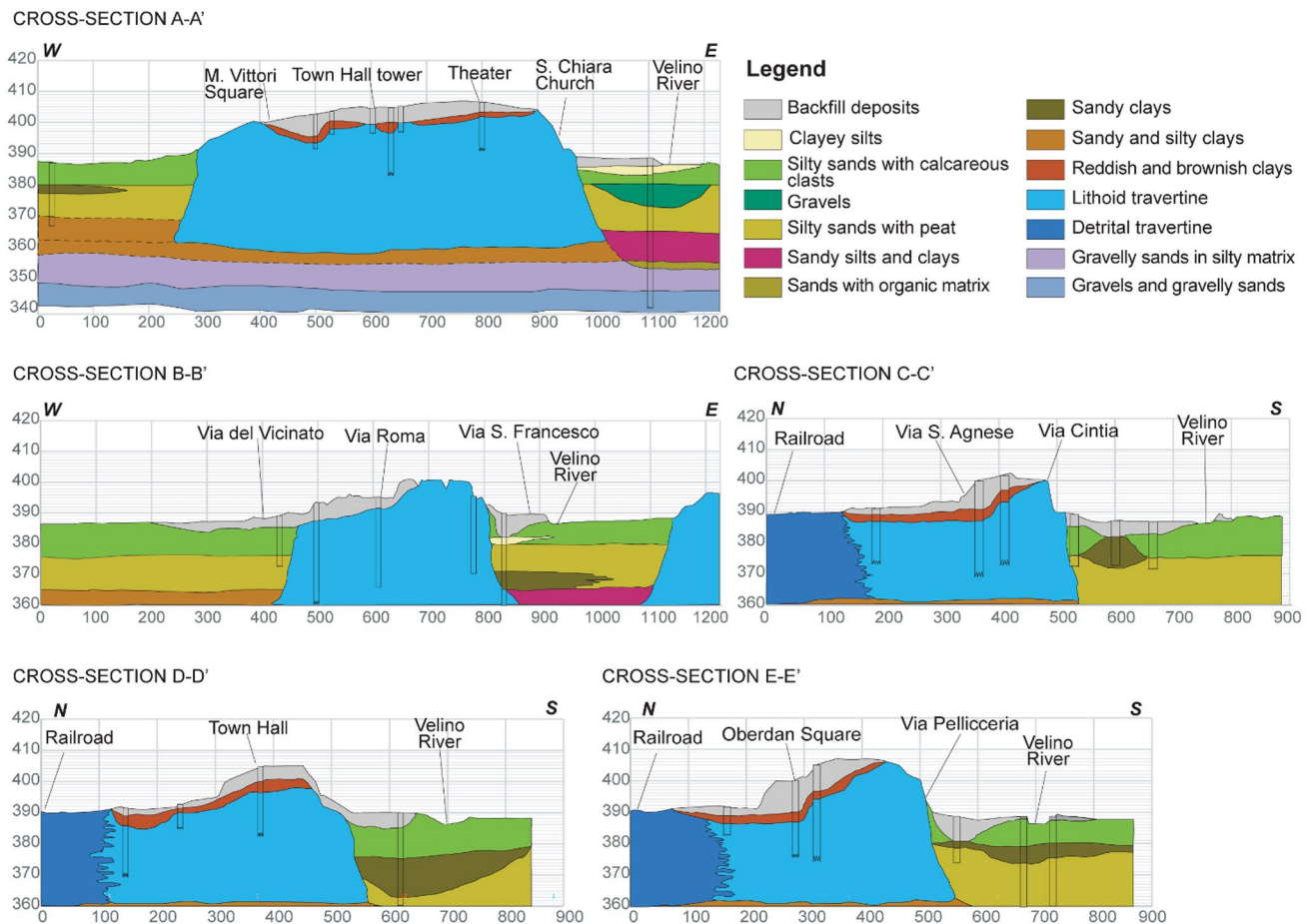


Fig. 6 Conceptual geological model of Rieti test site (vertical exaggeration factor of 5.5): **a** geological cross sections in the west–east direction and **b** geological cross sections in the north–south direction. For cross-section traces, see Fig. 4

In the westernmost sector of the A-A' cross section, the travertine platform ends steeply in contact with alluvial sediments. In the northern part of the city of Rieti, the lithoid travertine passes by heteropic contacts to the detrital travertine formation, as can be seen in the cross sections with N–S orientation (Fig. 6).

The 3D geological model describes the spatial relationships between the different geological bodies and the latero-vertical variations of the lithologies, and more specifically, it represents the geometry of the contacts of

the travertine platform both with the assumed underlying sandy and clayey levels and with the bordering alluvial deposits of the Velino River.

The extrapolation of 2D cross sections from the 3D solid model reveals the qualitative match of a traditional 2D and the 3D modeling approach in the reconstruction of the subsurface geological architecture. The model and cross sections depicted in Fig. 7 employ a vertical exaggeration factor of 10 to highlight the lithologic transitions.

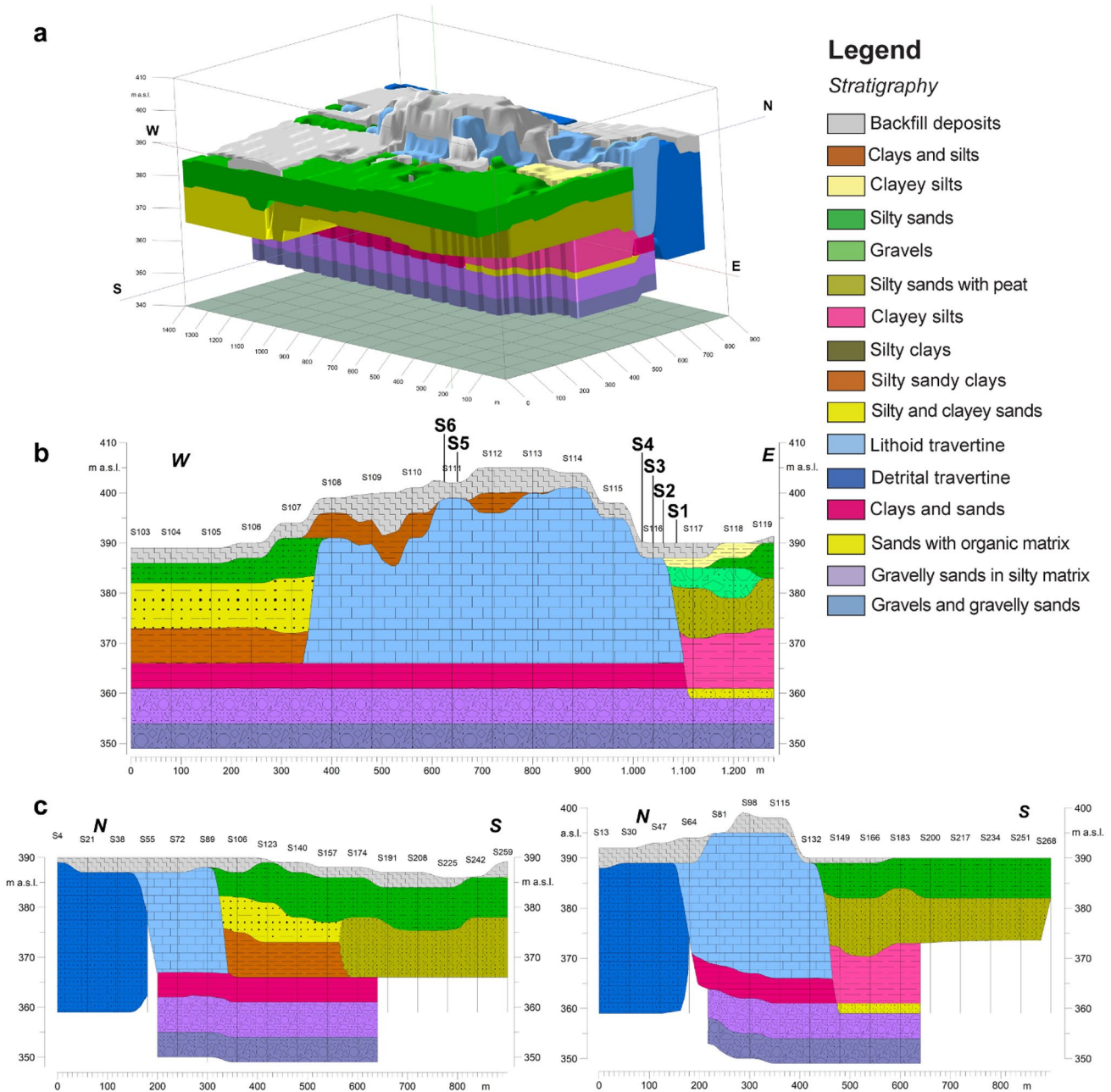


Fig. 7 a Three-dimensional engineering-geological model of Rieti city and (b) WE and (c) NS cross sections extrapolated from the 3D model. Projected location of the new validation boreholes S1, S2, S3, S4, S5, and S6 on b

Discussion

The 3D model of the subsoil allows the representation of entire volumes of subsurface through a solid restitution, unlike the traditional 2D approaches (maps and cross sections), which miss large areas, without providing an overall interpretation. For this reason, this model is easier to understand than traditional mapping products, offering a more intuitive mode of visualization that is accessible not only to technical specialists. Moreover, the geodatabase of the 3D solid model integrates all available geological and geophysical data into a single overview and can be quickly updated as new information becomes available and allows a rapid qualitative/quantitative analysis. The different parts of the model can be visualized separately, and it is possible to obtain information on the extent of the surfaces and volumes of the units as well as their spatial distribution. Finally, the digital output can be queried for interchangeability and specific analysis, such as the model validation.

Good adherence to the geological conceptual model is highlighted by the comparison with the validated cross section with WE direction (cross-section A-A' in Fig. 6), with the corresponding cross section extracted from the 3D model represented in Fig. 7b. As regards the cross sections trending NS (Fig. 7c), the ones extracted from the solid model provide the subsoil reconstruction up to greater depths, not reached by the boreholes, and therefore not included in the initial geological cross sections.

The accuracy of the 3D model has been verified through the acquisition of new data on the stratigraphy of Rieti subsoil, which were obtained after the construction of the 3D model. A set of new boreholes made it possible to compare the stratigraphic logs with the corresponding stratigraphic column extracted from the 3D model (Fig. 8), to perform a posteriori validation of the accuracy of the model. The new boreholes used are located in two areas: the first group of 4 surveys (boreholes S1, S2, S3, and S4) occurs at the Santa Chiara church, at the southwestern edge of the travertine platform (location in Figs. 4 and 7b), that represents the most crucial and complex zone of the geological model. The second group (boreholes S5 and S6) is in the center of the study area, at the town hall of Rieti, on the top of the travertine platform (location in Figs. 4 and 7b). In general, we can address that, as expected, the columns extracted from the 3D model show a more simplified stratigraphy, since the lithological units used in the construction of the geodatabase derive from a reasoned subdivision of the existing lithologies.

As regards S5 and S6, on the top of the travertine platform, a pretty good correspondence was verified between the new boreholes and the model created previously (the example of S5 is shown in Fig. 8). As regards S1, S2, S3,

and S4 at Santa Chiara church, the validation procedure revealed interesting details on 3D modeling of the edge of the travertine platform: S1 and S2 boreholes shown in Fig. 8 represent two different results of comparison between the 3D model, despite that the two boreholes are located only about 19 m apart. In the case of S1 (Fig. 8), a very good correlation between the new boreholes and the stratigraphic columns extracted from the 3D model was observed. Conversely, in the case of S2, a difference between the real borehole and the one extracted from the model stands out, as the latter shows 2.5 m of the alluvial sediments of Velino River (sands, gravels, and silts) between travertine and backfill deposits, that are missing in the real S2 borehole (Fig. 8). In other words, the column extracted from the 3D model reveals a small mistake in the modelling that corresponds to 2.5 m of thickness. As the sampling vertical step used in the geodatabase (synthetic boreholes) was 5 m, the error of 2.5 m is below the sampling step size and therefore cannot be avoided for this vertical resolution. Lastly, the S3 and S4 columns extracted from the 3D model demonstrate a better adherence to the validation boreholes.

To conclude, the validation of the model through the new boreholes shows that the very steep edges of the travertine platform and the abrupt contact with the alluvial sediments represent the most difficult part to be perfectly depicted by the 3D model, because in a very narrow area (distance from S1 to S2 of the order of 19 m), the geological structure of the subsoil changes abruptly, passing from the travertine platform to the alluvial valley. In this border zone, a small deviation (below the sampling step size) of the model from the real setting of the subsoil cannot be avoided with the adopted vertical resolution.

The 3D geological model can represent a useful tool for local seismic response studies as it allows the observation of the spatial relationships between different geological bodies and the latero-vertical variations of the lithologies at depth. In urban environments with complex and peculiar geological settings, such as the Rieti city center where the contacts between travertine formation and alluvial deposits cannot be directly observed on-site, the representation provided by the model can be very helpful in the perspective of local-scale studies of seismic response. In fact, the presence of a lateral variation between the travertine stiff rock and the alluvial soft soils can induce variation of the seismic ground motion due to the different physical and mechanical features of these two means, causing possible amplification effects in the areas located in the lateral parts of the alluvial valley, i.e., in proximity to the travertine platform buried edge.

Considering such a geological setting, comparable to a valley filled with recent soft soils bordered by a stiff seismic bedrock, similar seismic response schemes can be applied to the Rieti site. Using the approach proposed by Bard

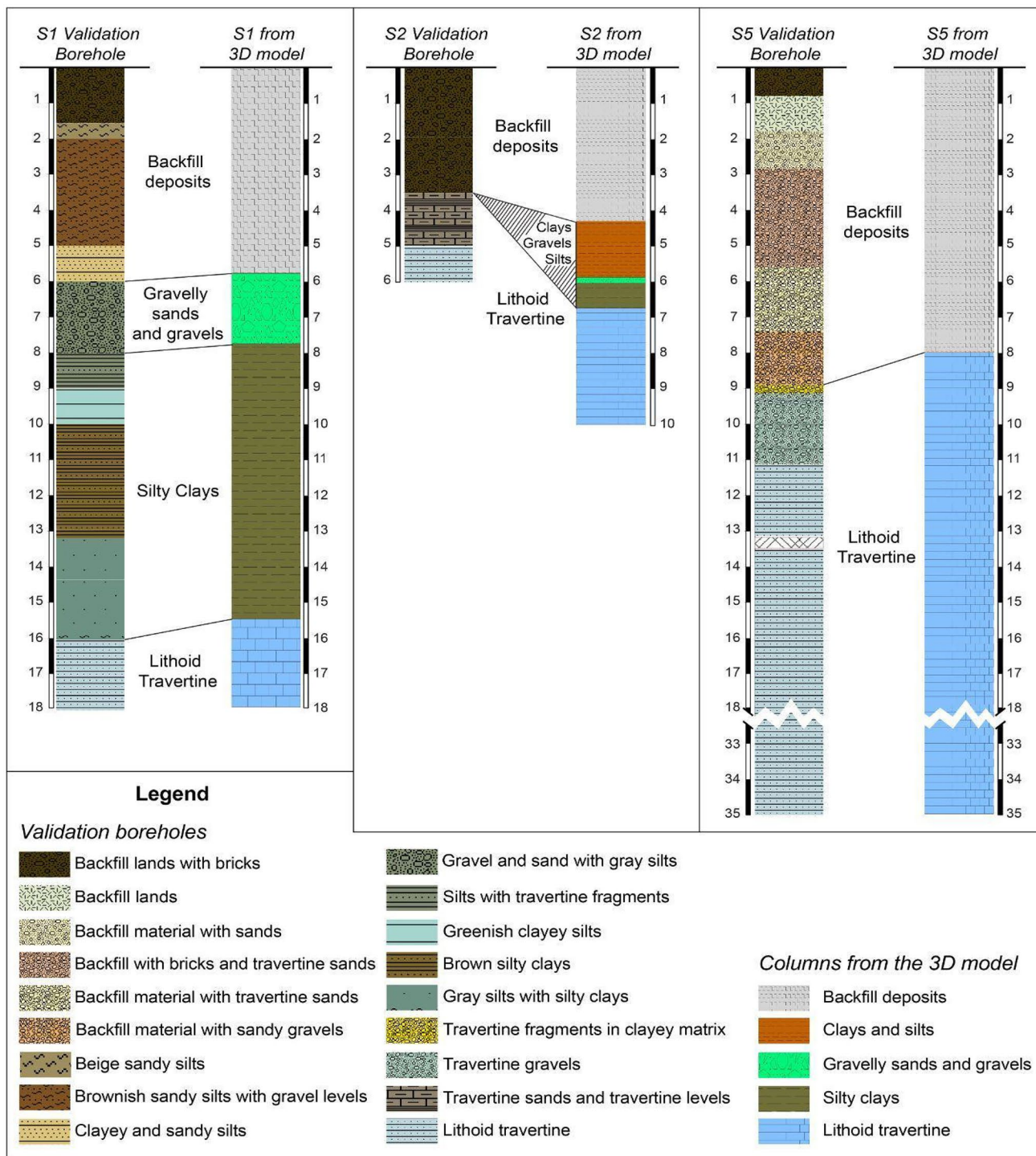
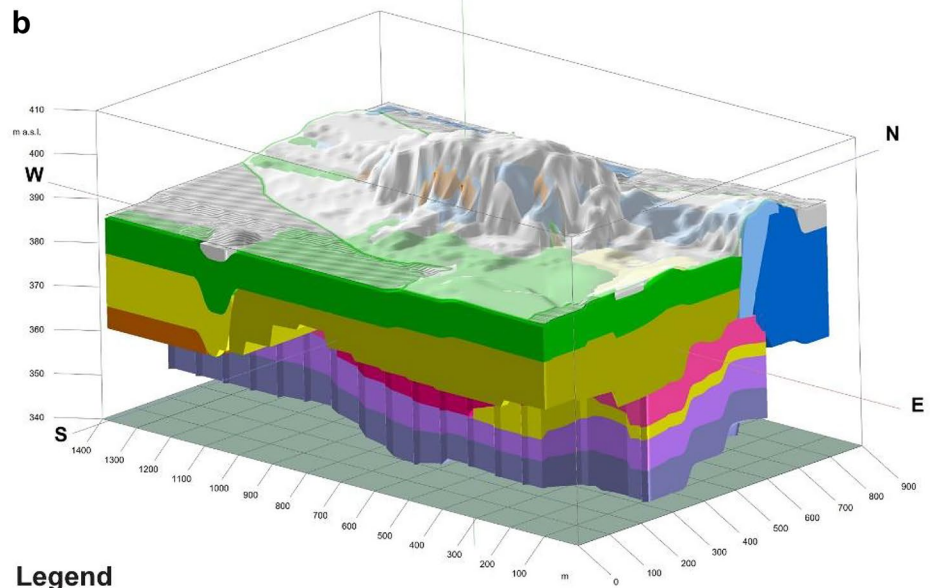


Fig. 8 A posteriori validation of the 3D model accuracy: new boreholes (location in Figs. 4 and 7b) compared with the corresponding stratigraphic columns extracted from the 3D model

and Bouchon (1985), the seismic response of a sedimentary valley can be associated with a 1D or 2D resonance scheme based on the impedance contrast between soft-soil and seismic bedrock, and on the geometrical shape. A 1D-like resonance is typical of a large valley while a 2D

resonance characterizes narrow ones. In case of a 1D resonance scheme, the resonance frequency value varies along the valley and depends on the thickness and mean V_s value of the filling deposits, except for the lateral parts where an additional contribution of lateral waves exists and where a

Fig. 9 Map (a) and 3D solid model (b) indicating zones with 1D and 2D seismic response schemes in the Rieti historical center (green and red colors, respectively, in transparency)



Legend

Stratigraphy

- | | |
|-----------------------|--------------------------------|
| Backfill deposits | Silty sandy clays |
| Clays and silts | Silty and clayey sands |
| Clayey silts | Lithoid travertine |
| Silty sands | Detrital travertine |
| Gravels | Clayey silts |
| Silty sands with peat | Sands with organic matrix |
| Clays and sands | Gravelly sands in silty matrix |
| Silty clays | Gravels and gravelly sands |

Suitable seismic response model

- | |
|----|
| 1D |
| 2D |

2D approach could be preferable with respect to a simplified 1D approach, especially if marked lateral heterogeneities are present in the filling deposits (Martino et al. 2015). In the case of a 2D resonance scheme, the resonance frequency is the same across the whole valley, associated with a significant amplification (up to 4 times the theoretical 1D value) and with an increased duration of the seismic motion.

Considering these assumptions and the latero-vertical variations of the lithologies at depth observed by the 3D geological model, a map distinguishing 1D and 2D resonance scheme zones was produced for the Rieti historical center (Fig. 9a), where a 2D modeling approach results preferable for the areas located on the top of the travertine plate and for the lateral part of the valley, while a simplified 1D modeling approach can be chosen for the areas located in the central part of the valley. In addition, the 3D geological model (Fig. 9b) can be used to extract seismostratigraphic columns or cross sections.

Conclusion

The 3D representation of the subsoil is increasingly used in many fields of application in Earth sciences, and it is becoming integrated into the common practices of representations of geological features, such as lithological bodies that resemble their real shape and size. Among the aforementioned applications, there is certainly the seismic risk management framework, and specifically the local seismic response analysis and the evaluation of the related seismic amplification. Such studies require indeed a reliable and high-resolution engineering-geological model of the subsoil.

This study shows a methodology that starts from scattered and predominantly punctual information on geology and synthesizes a 3D model of the subsoil. The experienced methodology involves three steps: (i) a conceptual geological model was obtained from data and maps of literature; (ii) an analysis of geophysical data (i.e., inversion of HVSR curves) allowed to validate this preliminary geological model infers the shear wave velocity values for the litotechnical units, and retrieves some additional stratigraphies for the construction of a larger geodatabase; and (iii) a 3D model was achieved by the geodatabase built on the basis of the previous steps. The accuracy of the 3D model can be verified a posteriori through the acquisition of new borehole stratigraphies in the study area, which can be compared with the corresponding stratigraphies obtained by querying the solid model.

The test area has been the historical city center of Rieti, where the subsoil is characterized by a peculiar local geological setting with the occurrence of a travertine platform that crops out in the historic city center. The a posteriori validation phase highlighted a good adherence of the 3D model to the new boreholes stratigraphies and made it possible to point out

some limits of the 3D modeling in the representation of abrupt lateral discontinuities, such as the edges of the travertine platform. Generally speaking, the limitations of 3D geomodeling lie in the need for a large amount of data to reconstruct a robust engineering-geological model and capture the variability of complex geobodies. Exploiting classical geological information and coupling virtual surveys to real data can potentially bridge the gap in quantitative and qualitative data availability.

The engineering-geological model can support properly the localization of possible condition where local seismic effects may occur in case of an earthquake. The model suggests the zones where a 2D modeling approach better represents the local site seismic response and the zones where a 1D modeling approach is suitable. The relevant lateral heterogeneities between the stiff travertine, characterized by relatively high S-wave velocity values, and the alluvial soft soils in the lateral parts of the buried fluvial valley of the Velino river, represent a particular setting regarding the seismic site characterization, due to possible contributions of lateral waves reflected from scatters which coincide with the seismic bedrock boundaries. For future studies, considering the latero-vertical variations of the lithologies and the different expected amplification effects, specific cross sections can be extracted from the 3D geological model to perform numerical simulations of seismic wave propagation, based on the proper modeling approach for each specific areas of interest.

Acknowledgements This work has been developed in the framework of the H2020-RISE, Num. 823966, STABLE (Structural stABLity risk assEsmnt) project (www.stable-project.eu). The authors wish to thank the municipality of Rieti, Dr. Geol. Matteo Carrozzoni for supporting this study, and Dr. Jessica Clementi for her suggestions regarding Rieti's historical background.

Author contribution Conceptualization: Benedetta Antonielli and Francesca Bozzano. Methodology: Roberto Iannucci and Paolo Ciampi. Formal analysis and investigation: Benedetta Antonielli, Roberto Iannucci, Paolo Ciampi, and Federico Giudici. Writing—original draft preparation: Benedetta Antonielli, Roberto Iannucci, and Paolo Ciampi. Writing—review and editing: Salvatore Martino, Domenico Marchetti, Benedetta Antonielli, Roberto Iannucci, and Paolo Ciampi. Funding acquisition: Francesca Bozzano. Supervision: Francesca Bozzano and Gabriele Scarascia Mugnozza.

Funding Open access funding provided by Università degli Studi di Roma La Sapienza within the CRUI-CARE Agreement. The in-situ survey and the analysis have been developed thanks to funding from the H2020-RISE, Num. 823966, STABLE (Structural stABLity risk assEsmnt) project (www.stable-project.eu).

Declarations

Conflict of interest The authors declare no competing interests.

Open Access This article is licensed under a Creative Commons Attribution 4.0 International License, which permits use, sharing, adaptation, distribution and reproduction in any medium or format, as long as you give appropriate credit to the original author(s) and the source, provide a link to the Creative Commons licence, and indicate if changes

were made. The images or other third party material in this article are included in the article's Creative Commons licence, unless indicated otherwise in a credit line to the material. If material is not included in the article's Creative Commons licence and your intended use is not permitted by statutory regulation or exceeds the permitted use, you will need to obtain permission directly from the copyright holder. To view a copy of this licence, visit <http://creativecommons.org/licenses/by/4.0/>.

References

- Aghamolaie I, Lashkaripour GR, Ghafoori M, Moghaddas NH (2019) 3D geotechnical modeling of subsurface soils in Kerman city, southeast Iran. *Bull Eng Geol Environ* 78:1385–1400. <https://doi.org/10.1007/s10064-018-1240-7>
- Alvino G, Lezzi F (2013) Reate/Rieti. *Archeologia Urbana*, in Lazio e Sabina 9:145–150
- Alvino G, Lezzi F (2016) Il paesaggio urbano di Rieti: presenze antiche ritrovate. *Lazio e Sabina* 11:243–245
- Antonielli B, Bozzano F, Fiorucci M, Hailemichael S, Iannucci R, Martino S, Rivellino S, Scarascia Mugnozza G (2021) Engineering-geological features supporting a seismic-driven multi-hazard scenario in the Lake Campotosto area (L'Aquila, Italy). *Geosciences* 11(3):107
- Arenas-Abad C, Vázquez-Urbez M, Pardo-Tirapu G, Sancho-Marcén C (2010) Fluvial and associated carbonate deposits. In: Alonso-Zarza AM, Tanner LH (eds) *Developments in sedimentology: carbonates in continental settings: facies, environments and processes*. Elsevier, Amsterdam, pp 133–175
- Archer C, Noble P, Rosen MR, Sagnotti L, Florindo F, Mensing S, Piovesan G, Michetti AM (2019) Lakes as paleoseismic records in a seismically-active, low-relief area (Rieti Basin, central Italy). *Quat Sci Rev* 211:186–207. <https://doi.org/10.1016/j.quascirev.2019.03.004>
- Baojun W, Bin S, Zhen S (2009) A simple approach to 3D geological modelling and visualization. *Bull Eng Geol Environ* 68:559. <https://doi.org/10.1007/s10064-009-0233-y>
- Bard PY, Bouchon M (1985) The two-dimensional resonance of sediment-filled valleys. *Bull Seismol Soc Am* 75(2):519–541
- Blumetti AM, Dramis F, Michetti AM (1993) Fault-generated mountain fronts in the central Apennines (Central Italy): Geomorphological features and seismotectonic implications. *Earth Surf Process Landf* 18(3):203–223
- Bour M, Fouissac D, Dominique P, Martin C (1998) On the use of microtremor recordings in seismic microzonation. *Soil Dyn Earthq Eng* 17(7–8):465–474
- Brunamonte F, Michetti AM, Serva L, Vittori E (1993) Seismic hazard evaluation in central Italy: preliminary results of the Rieti Basin project. *Ann Geofis* 36:253–262
- Calderini G, Calderoni G, Cavinato GP, Gliozzi E, Paccara P (1998) The upper Quaternary sedimentary sequence at Rieti Basin (central Italy): a record of sedimentation response to climatic changes. *Palaeogeogr Palaeoclimatol Palaeoecol* 140:97–111
- Calderoni G, Carrara C, Ferreli L, Follieri M, Gliozzi E, Magri D, Narcisi B, Parotto M, Sadori L, Serva L (1994) Palaeoenvironmental, palaeoclimatic and chronological interpretations of a late Quaternary sediment core from Piana di Rieti (central Apennines, Italy). *G Geol* 3 56(2):43–72
- Camerieri P (2009) La ricerca della forma del catasto antico di Reate nella pianura di Rosea. In: Coarelli F, De Santis A (eds) *Reate e l'Ager Reatinus. Vespasiano e la Sabina: dalle origini all'impero*, pp. 39–48, Quasar. (in Italian)
- Camerieri P, Mattioli T (2014) Archeologia e modificazioni ambientali lungo il corso del fiume Velino. In: Aversa M, Colapietro A, Nisio S, Ventura G (eds) *Memorie descrittive carta geologica d'Italia*, vol 96, SELCA, pp 169–188 (in Italian)
- Capuzzoli E, Gandin A, Sandrelli F (2008) Evidence of associated deposition of travertine and calcareous tufa in the Quaternary carbonates of Valdelsa Basin (Tuscany). *Ital J Quatern Sci* 21:113–124
- Carminati E, Lustrino M, Doglioni C (2012) Geodynamic evolution of the central and western Mediterranean: Tectonics vs. igneous petrology constraints. *Tectonophysics* 579:173–192
- Carrara C, Brunamonte F, Ferreli L, Lorenzoni P, Margheriti L, Michetti AM, Raglione M, Rosati M, Serva L (1992) I terrazzi della medio-bassa valle del F. Velino. In: Farabollini P, Invernizzi C, Pizzi A, Cavinato GP, Miccadei E (eds) *Evoluzione geomorfologica e tettonica quaternaria dell'Appennino centro-meridionale*, vol 1992/1. *Studi Geologici Camerti*, Università degli Studi di Camerino, pp 39–53 (in Italian)
- Carrara C, Esu D, Ferreli L (1995) Lo sbarramento di travertino delle Marmore (Bacino di Rieti, Italia Centrale): aspetti geomorfologici, faunistici ed ambientali. *Alpine and Mediterranean Quaternary* 8(1):111–118. (in Italian)
- Carrara C, Ferreli L, Guerrini L, Serva L (2004) The Rieti Inter-mountain Basin and S. Francesco D'Assisi. 32nd International Geological Congress, Florence, Italy, 20–28 August 2004, pp 20–28
- Cavinato G, De Celles P (1999) Extensional basins in the tectonically bimodal central Apennines fold-thrust belt, Italy: response to corner flow above a subducting slab in retrograde motion. *Geology* 27(10):955–958
- Chiaraluce L, Di Stefano R, Tinti E, Scognamiglio L, Michele M, Casarotti E, Cattaneo M, De Gori P, Chiarabba C, Monachesi G, Lombardi A, Valoroso L, Latorre D, Marzorati S (2017) The 2016 Central Italy seismic sequence: a first look at the mainshocks, aftershocks, and source models. *Seismol Res Lett* 88:757–771. <https://doi.org/10.1785/0220160221>
- Ciampi P, Esposito C, Bartsch E, Alesi EJ, Petrangeli Papini M (2021) 3D dynamic model empowering the knowledge of the decontamination mechanisms and controlling the complex remediation strategy of a contaminated industrial site. *Sci Total Environ* 793:148649. <https://doi.org/10.1016/j.scitotenv.2021.148649>
- Ciampi P, Esposito C, Cassiani G, Deidda GP, Flores-Orozco A, Rizzetto P, Chiappa A, Bernabei M, Gardon A, Papini MP (2022) Contamination presence and dynamics at a polluted site: Spatial analysis of integrated data and joint conceptual modeling approach. *J Contam Hydrol* 248:104026
- Colombi A, Hailemichael S, Martini G, Martino S, Paciello A, Peloso A, Salvatori L, Scarascia Mugnozza G, Verrubbi V (2013) Studies of seismic microzonation in Latium region (Italy) by experiencing the application of official guidelines in intra-mountain plains. In: Brebbia CA, Hernández S (eds) *Earthquake Resistant Engineering Structures*. WIT Press, pp 35–45
- Colombi A, Hailemichael S, Martini G, Martino S, Paciello A, Peloso A, Salvatori L, Scarascia Mugnozza G, Verrubbi V (2015) The experience of seismic microzonation in Lazio Region (Italy) mountain municipalities. In: Lollino G, Manconi A, Guzzetti F, Culshaw M, Bobrowsky P, Luino F (eds) *Engineering Geology for Society and Territory*, vol 5. Springer, pp 1101–1105
- Colombi A, Hailemichael S, Martini G, Martino S, Paciello A, Paolini SL (2011) Studi di risposta sismica locale nelle aree urbane di piana alluvionale: il caso di Rieti. In: Scarascia Mugnozza G (ed) *La Pericolosità Sismica nel Lazio*, Italian Journal of Engineering Geology and Environment - Book Series. Casa Editrice Università La Sapienza, pp 171–179 (ISBN: 9788895814612, in Italian)
- Comerci V, Molin D, Pasquarè FA, Serva ML (2003) Risposta sismica dell'area urbana di Rieti in occasione del terremoto del 27 giugno 1898 nel bacino di Vazia (RI). *Boll Soc Geol Ital* 122:147–156 (in Italian)

- Cosentino D, Parotto M (1992) La struttura a falde della Sabina (Appennino centrale). In: Tozzi M, Cavinato GP, Parotto M (eds) Studi preliminari all'acquisizione dati del profilo CROP 11 Civitavecchia-Vasto, vol 1991/2. Studi Geologici Camerti, Università degli Studi di Camerino, pp 381–387 (in Italian)
- D'Agostino N, Jackson JA, Dramis F, Funicciello R (2002) Interactions between mantle upwelling, drainage evolution and active normal faulting: an example from the central Apennines (Italy). *Geophys J Int* 147(2):475–497
- Doglioni C (1993) Some remarks on the origin of the foredeeps. *Tectonophysics* 228:1–20
- Ferrelli L, Brunamonte F, Filippi G, Margheriti L, Michetti AM (1992) Riconoscimento di un livello lacustre della prima età del ferro nel bacino di Rieti e possibili implicazioni neotettoniche. In: Farabollini P, Invernizzi C, Pizzi A, Cavinato GP, Miccadei E (eds) Evoluzione geomorfologica e tettonica quaternaria dell'Appennino centro-meridionale. Studi Geologici Camerti, vol. spec. 1992/1, pp. 127–135, Università degli Studi di Camerino. (in Italian)
- Galli P, Castenetto S, Peronace E (2017) The macroseismic intensity distribution of the 30 October 2016 earthquake in Central Italy (Mw 6.6): seismotectonic implications. *Tectonics* 36:2179–2191
- Gandin A, Capezzuoli E (2008) Travertine versus Calcareous tufa: distinctive petrologic features and stable isotope signatures. *Ital J Quatern Sci* 21:125–136
- Gaudiosi I, Del Monaco F, Milana G, Tallini M (2014) Site effects in the Aterno River Valley (L'Aquila, Italy): comparison between empirical and 2D numerical modelling starting from April 6th 2009 Mw 6.3 earthquake. *Bull Earthq Eng* 12(2):697–716
- Guerrieri L, Comerci V, Ferrelli L, Pompili R, Serva L, Brunamonte F, Michetti AM (2006) Geological evolution of the intermountain Rieti Basin (central appennines). In: Pasquarè G, Venturini C, Gropelli G (eds) Mapping Geology in Italy. APAT-Servizio Geologico d'Italia, SELCA, pp 123–130
- Guerrieri L, Brunamonte F, Comerci V, Ferrelli L, Michetti AM, Pompili R, Serva L (2004) Geologic map of continental deposits in the Rieti Basin (Central Apennines). In: Pasquarè G, Venturini C (eds) Mapping geology in Italy. SELCA, pp 123–130
- Guo J, Wang X, Wang J, Dai X, Wu L, Li C, Li F, Liu S, Jessell MW (2021) Three-dimensional geological modeling and spatial analysis from geotechnical borehole data using an implicit surface and marching tetrahedra algorithm. *Eng Geol* 284:106047. <https://doi.org/10.1016/j.enggeo.2021.106047>
- Haghshenas E, Bard PY, Theodulidis N (2008) Empirical evaluation of microtremor H/V spectral ratio. *Bull Earthq Eng* 6(1):75–108
- He H, He J, Xiao J et al (2020) 3D geological modeling and engineering properties of shallow superficial deposits: a case study in Beijing, China. *Tunn Undergr Sp Technol* 100:103390
- Iannucci R, Antonielli B, Coradini M, Karastathis V, Maniatakis C, Martino S, Messina L, Mouzakiotis E, Paciello A, Rivellino S, Saroglou C, Bozzano F (2022) Analysis of the local seismic response in the Strovolos Municipality (Nicosia District, Cyprus). *Italian J Eng Geol Environ* 1:43–53
- ICMS Working Group (2008) Indirizzi e criteri per la microzonazione sismica - Guidelines for seismic microzonation. Conferenza delle Regioni e delle Province autonome. Dipartimento della Protezione Civile. <https://www.centromicrozonazioneismica.it/it/download/category/3-linee-guida> Access date April 2022
- ITHACA Working Group (2019) ITHACA (ITaly HAZard from Capable faulting) A database of active capable faults of the Italian territory. Version December 2019. ISPRA. Web Portal <http://sgi2.isprambiente.it/ithacaweb/Mappatura.aspx> Access date April 2022
- Kanlı AI, Tildy P, Pronay Z, Pınar A, Hermann L (2006) VS30 mapping and soil classification for seismic site effect evaluation in Dinar Region, SW Turkey. *Geophys J Int* 165(1):223–235
- Kanlı AI, Kang TS, Pınar A, Tildy P, Pronay Z (2008) A systematic geophysical approach for site response of the Dinar Region, South Western Turkey. *J Earthquake Eng* 12(S2):165–174
- Kanlı AI (2010) Integrated approach for surface wave analysis from near-surface to bedrock. In: Miller RD, Bradford JD, Holliger K (Eds) Advances in near-surface seismology and ground-penetrating radar, Geophysical developments series No. 15, SEG Reference Publications, Society of Exploration Geophysicists, American Geophysical Union and Environmental and Engineering Geophysical Society, Tulsa (Oklahoma, US), Chapter 29, pp. 461–476. <https://doi.org/10.1190/1.9781560802259.ch29>
- Liu H, Chen S, Hou M, Liang H (2020) Improved inverse distance weighting method application considering spatial autocorrelation in 3D geological modeling. *Earth Sci Inform* 13:619–632. <https://doi.org/10.1007/s12145-019-00436-6>
- Locati M, Camassi R, Rovida A, Ercolani E, Bernardini F, Castelli V, Caracciolo CH, Tertulliani A, Rossi A, Azzaro R, D'Amico S, Antonucci A (2022) Database Macrosismico Italiano (DBMI15). Vers. 4.0. INGV. <https://doi.org/10.13127/DBMI/DBMI15.4>
- Lorenzoni P, Raglione M, Brunamonte F, Michetti AM, Pennacchioni M (1993) Stratigrafia dei depositi di versante tardo-quaternari del Bacino di Rieti: la sezione de "La Casetta". In: Farabollini P, Invernizzi C, Pizzi A, Cavinato GP, Miccadei E (ed) Evoluzione geomorfologica e tettonica quaternaria dell'Appennino centro-meridionale, vol 1992/1. Studi Geologici Camerti, Università degli Studi di Camerino, pp 145–153 (in Italian)
- Lustrino M, Luciani N, Stagno V, Narzisi S, Masotta M, Scarlato P (2022) Experimental evidence on the origin of Ca-rich carbonated melts formed by interaction between sedimentary limestones and mantle-derived ultrabasic magmas. *Geology* 50(4):476–480. <https://doi.org/10.1130/G49621.1>
- Macerola L, Tallini M, Di Giulio G, Nocentini M, Milana G (2019) The 1-D and 2-D Seismic modeling of deep quaternary basin (Downtown L'Aquila, Central Italy). *Earthq Spectra* 35(4):1689–1710
- Madera GA (1970) Fundamental period and amplification of peak acceleration in layered systems. MIT Department of Civil Engineering, Inter-American Program
- Madonna S, Nisio S, Gandin A (2020) Le cavità nascoste nei "calcareous tufa" del sottosuolo di Rieti. *Memorie Descrittive Della Carta Geologica D'italia* 107:357–382 (in Italian)
- Martino S, Lenti L, Gélis C, Giacomi AC, Santisi d'Avila MP, Bonilla LF, Bozzano F, Semblat JF (2015) Influence of lateral heterogeneities on strong-motion shear strains: simulations in the historical center of Rome (Italy). *Bull Seismol Soc Am* 105(5):2604–2624
- Michetti AM, Brunamonte F, Serva L, Whitney RA (1995) Seismic hazard assessment from paleoseismological evidence in the Rieti Region (Central Italy). In: Serva L, Burton D (eds) Perspectives in Paleoseismology, Bulletin of the Association of Engineering Geologists Special Publication, vol 6. Peanut Butter Publishing, pp 63–82
- Moscattelli M, Albarello D, Scarascia Mugnozza G, Dolce M (2020) The Italian approach to seismic microzonation. *Bull Earthq Eng* 18(12):5425–5440
- Moscattelli M, Vignaroli G, Pagliaroli A, Razzano R, Avalle A, Gaudiosi I, Giallini S, Mancini M, Simionato M, Sirianni P, Sottili G, Bellanova J, Calamita G, Perrone A, Piscitelli S, Lanzo G (2021) Physical stratigraphy and geotechnical properties controlling the local seismic response in explosive volcanic settings: the Stracciaccappa maar (central Italy). *Bull Eng Geol Environ* 80(1):179–199
- Nakamura Y (1989) A method for dynamic characteristics estimation of subsurface using microtremor on the ground surface. *Q Rep Rail Tech Res Inst* 30:25–30
- Oubaiche EH, Chatelain JL, Bouguern A, Bensalem R, Machane D, Hellel M, Khaldouy B, Guillier B (2012) Experimental

- relationship between ambient vibration H/V peak amplitude and shear-wave velocity contrast. *Seismol Res Lett* 83(6):1038–1046
- Patacca E, Sartori R, Scandone P (1992) Tyrrhenian basin and Apenninic arcs: kinematic relations since late Tortonian times. *Mem Soc Geol It* 45:425–451
- Pedley M, González Martín JA, Ordonèz Delgado S, Garcia Del Cura MA (2003) Sedimentology of Quaternary perched springline and paludal tufas: criteria for recognition, with examples from Guadalajara Province, Spain. *Sedimentology* 50:23–44
- Pergalani F, Pagliaroli A, Bourdeau C, Compagnoni M, Lenti L, Lualdi M, Madiari C, Martino S, Razzano R, Varone C, Verrubbi V (2020) Seismic microzoning map: approaches, results and applications after the 2016–2017 Central Italy seismic sequence. *Bull Earthq Eng* 18(12):5595–5629
- Rovida A, Locati M, Camassi R, Lolli B, Gasperini P, Antonucci A (2022) Catalogo Parametrico dei Terremoti Italiani (CPTI15), ver. 4.0. INGV. <https://doi.org/10.13127/CPTI/CPTI15.4>
- Royse KR, Rutter HK, Entwisle DC (2009) Property attribution of 3D geological models in the Thames Gateway, London: new ways of visualising geoscientific information. *Bull Eng Geol Environ* 68:1–16
- Scarascia Mugnozza G, Martino S, Salvatori L, Porchia A, Martini G, Paciello A, Paolini S, Peloso A, Verrubbi V, Hailemichael S (2013) Relazione illustrativa microzonazione sismica livello 1 Comune di Rieti. <https://www.comune.rieti.it/content/microzonazione-sismica-livello-1> (in Italian)
- Serpenti M, Carlucci R, Di Iorio A, Bozzano F, Antonielli B, Martino S, Charalampopoulou B, Kontopoulos C, Fokaidis P, Christou P, Papadopoulos N, Saroglou H, De Angeli S (2020) Stable: structural stability risk assessment. 8th International Conference on Remote Sensing and Geoinformation of the Environment (RSCy2020), Paphos, Cyprus, 16–18 March 2020, SPIE, vol 11524, pp 120–128
- SESAME (2004) Guidelines for the implementation of the H/V spectral ratio technique on ambient vibrations-Measurements, processing and interpretation. SESAME European research project, Deliverable D23. 12., Project No. EVG1-CT-2000-00026 SESAME
- Skrame K, Di Filippo M, Di Nezza M (2018) New gravimetric map of the Rieti intra-mountain basin (Central Apennines, Italy), vol 2018. 24th European Meeting of Environmental and Engineering Geophysics, Porto, Portugal, 9–12 September 2018, pp 1–5. <https://doi.org/10.3997/2214-4609.201802539>
- Soligo M, Tuccimei P, Barberi R, Delitala MC, Miccadei E, Taddeucci A (2002) U/Th dating of freshwater travertine from Middle Velino Valley (Central Italy): paleoclimatic and geological implications. *Palaeogeogr Palaeoclimatol Palaeoecol* 184:147–216
- Sonmez YB, Celiker M, Bas S (2019) An investigation on the evaluation of dynamic soil characteristics of the Elazig City through the 1-D equivalent linear site-response analysis. *Bull Eng Geol Environ* 78(7):4689–4712
- Stoppa F, Villa IM (1991) Primi dati cronologici del distretto ultracalcinico umbro-laziale. Workshop SIMP, Pisa, Italy, 12–13 Luglio 1991 (in Italian)
- Tallini M, Lo Sardo L, Spadi M (2020) Seismic site characterisation of Red Soil and soil-building resonance effects in L'Aquila downtown (Central Italy). *Bull Eng Geol Environ* 79(8):4021–4034
- Tunar Özcan N, Ulusay R, Işık NS (2019) Assessment of dynamic site response of the peat deposits at an industrial site (Turkey) and comparison with some seismic design codes. *Bull Eng Geol Environ* 78(4):2215–2235
- Varone C, Lenti L, Martino S, Semblat JF (2021) Spatial variability of the urban ground motion in a highly heterogeneous site-city configurations. *Bull Earthq Eng* 19(1):27–45
- Zhang Q, Zhu H (2018) Collaborative 3D geological modeling analysis based on multi-source data standard. *Eng Geol* 246:233–244
- Zhu LF, Li MJ, Li CL, Shang JG, Chen GL, Zhang B, Wang XF (2013) Coupled modeling between geological structure fields and property parameter fields in 3D engineering geological space. *Eng Geol* 167:105–116